

Damage assessment and performance-based seismic design of timber-steel hybrid shear wall systems

Zheng Li^{*1,2}, Minjuan He¹, Minghao Li² and Frank Lam²

¹Department of Building Engineering, Tongji University, Shanghai, 200092, China

²Department of Wood Science, University of British Columbia, Vancouver, V6T 1Z4, Canada

(Received March 2, 2014, Revised March 30, 2014, Accepted April 3, 2014)

Abstract. This paper presents a reliability-based analysis on seismic performance of timber-steel hybrid shear wall systems. Such system is composed of steel moment resisting frame and infill wood frame shear wall. The performance criteria of the hybrid system with respect to different seismic hazard levels were determined through a damage assessment process, and the effectiveness of the infill wood shear walls on improving the seismic performance of the hybrid systems was evaluated. Performance curves were obtained by considering different target non-exceedance probabilities, and design charts were further established as a function of seismic weight. Wall drift responses and shear forces in wood-steel bolted connections were used as performance criteria in establishing the performance curves to illustrate the proposed design procedure. It was found that the presence of the infill wood shear walls significantly reduced the non-performance probabilities of the hybrid wall systems. This study provides performance-based seismic evaluations on the timber-steel hybrid shear walls in support of future applications of such hybrid systems in multi-story buildings.

Keywords: wood structures; timber-steel hybrid; shear walls; seismic design method; performance-based; performance criteria

1. Introduction

With the increasing urban density nowadays, attempts have been made to explore possible ways for the development of multi-story timber or timber-hybrid buildings. Feasibility analysis for innovative timber based multi-story building systems was conducted (Zhou *et al.* 2012; Dickof *et al.* 2012), and several structural prototype buildings were experimentally tested (Sakamoto *et al.* 2004; Buchanan *et al.* 2008; Smith *et al.* 2009; van de Lindt *et al.* 2010; Fragiaco *et al.* 2011; Ceccotti *et al.* 2013).

He *et al.* (2013) proposed a multi-story timber-steel hybrid building system which is composed of steel moment frames, infill wood frame shear walls, and timber-steel hybrid diaphragms. The infill wood frame shear walls are integrated in the steel moment frames by bolted connections. Experimental studies revealed that the infill wood shear walls were effective in resisting lateral loads in the hybrid system. However, more studies are needed to quantify the seismic performance

*Corresponding author, Ph.D. Candidate, E-mail: 09lizheng@tongji.edu.cn

of such a hybrid shear wall system before its more practical applications.

Performance-based or reliability-based seismic design represents a recent trend in the evolution of building design philosophies. Particularly, for newly developed building systems, performance-based seismic design represents a rational approach since the performance of new systems is not fully understood due to the lack of in field performance history or enough test data. For steel moment frames, performance-based analyses have been carried out by many researchers (e.g. Wang and Wen 2000; Kinali and Ellingwood 2007; Kazantzi *et al.* 2008, 2011). For wood shear walls, seismic reliability analyses have also been extensively conducted. Filiatrault and Folz (2002) proposed a framework for performance-based design of wood frame buildings, and a sample design procedure was also presented. Kim and Rosowsky (2004) proposed a fragility analysis methodology to evaluate the probable response of light wood frame construction subjected to different natural hazard levels, and a risk-based methodology was developed to guide the seismic design of 2.44 m by 2.44 m wood shear walls. Pang *et al.* (2010) introduced a simplified direct displacement design (DDD) procedure for multi-story wood frame buildings. Gu (2006) compared seismic reliabilities of Japanese wood shear walls constructed with three different wood species under three gravity load levels, and Li *et al.* (2009) studied the seismic reliability of Japanese diagonal-braced wood shear walls.

However, no research work has been reported on studying the seismic performance of timber-steel hybrid shear walls using reliability-based approaches. In this study, a performance-based seismic design procedure for timber-steel hybrid shear wall systems was presented. Performance criteria for the hybrid shear wall systems were defined according to a damage assessment process, and the seismic non-performance probability of the hybrid shear walls with respect to different seismic hazard levels was evaluated. The influence of design parameters, such as, the lateral infill-to-frame stiffness ratio, on the seismic performance was studied. Considering the seismic weight as a design variable, sample performance-based design charts in terms of peak wall drift response and shear forces in the wood-steel bolted connections were presented.

2. Damage analysis

For shear wall systems, it is commonly accepted that wall drift responses are able to provide a clear measurement of both structural and non-structural damages. The ASCE/SEI-41 has defined the structural performance levels with respect to immediate occupancy (IO), life safety (LS) and collapse prevention (CP) limit states, which are corresponding to different seismic hazard levels (earthquakes with exceedance probabilities of 50%, 10% and 2 % in a 50-year window for IO, LS and CP, respectively). It was found by He *et al.* (2013) that steel moment frames provided major contributions to lateral resistance for the timber-steel hybrid shear wall systems. However, the initial stiffness of the hybrid wall system was greatly increased due to the presence of the infill wood walls. For steel moment frames acting as lateral force resisting systems, it is recommended by ASCE/SEI-41 that the drift limits of 0.7%, 2.5% and 5.0% can be used as performance requirements for IO, LS and CP limit states, respectively. In the hybrid shear wall systems, the appropriateness of these drift limits was carefully validated through a detailed damage analysis. This has been done by investigating the relationship between the drift ratios and the structural damages of a full-scale 3 m by 6 m one-story timber-steel hybrid structure which was experimentally tested. Fig. 1 shows one of the hybrid shear wall systems in the test structure, and



Fig. 1 Test for timber-steel hybrid shear wall system

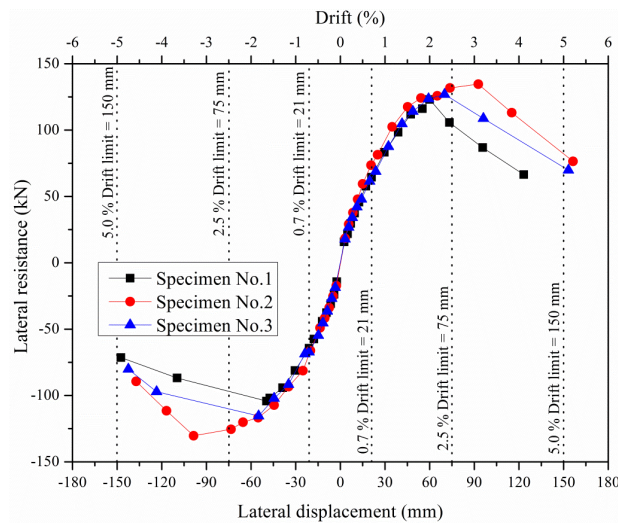


Fig. 2 Backbone load-displacement curves from the test



(a)



(b)

Fig. 3 Damage in the infill wood shear wall at: (a) LS limit state, and (b) CP limit state

Table 1. Structural performance levels for timber-steel hybrid shear wall systems

| Structural subsystem | Structural performance levels | | |
|------------------------|--|---|--|
| | Collapse prevention | Life safety | Immediate occupancy |
| Steel frame | Extensive distortion of steel beams and column panels. Many yielding zones / fractures at moment connections, but shear connections remain intact. | Plastic zones form in steel members. Local buckling of some beam elements. Joint distortion may occur, but shear connections remain intact. | Minor local yielding at a few places. |
| Infill wood shear wall | Failure of connection lines, nails withdrawn, some splitting of members and panels, and veneers dislodged. | Moderate loosening of connections and minor splitting in infill walls. Failures in corner nails. | No failures in wood sheathing-framing connections. Distributed minor hairline cracking of gypsum is allowed. |
| Drift limit | 5% transient or permanent | 2.5% transient or 1% permanent | 0.7% transient |

Fig. 2 shows the backbone load-displacement curves for the hybrid shear walls. Detailed information about these tests can be found in He *et al.* (2013).

According to ASCE/SEI-41, the IO performance level is defined as the post-earthquake damage state in which a structure remains safe to occupy, essentially retaining its pre-earthquake design strength and stiffness, and only minor local yielding in a few steel members is allowed. Strain gages were used to monitor the stress status of the steel members in the hybrid system tests. It was found that local yielding occurred in one of the beam-column joints at the drift ratio of 0.7 %, and yielding zones in the steel members began to form when the drift ratio exceeded 0.7 %. No failure was found in the infill wood shear walls. Therefore, the drift ratio of 0.7 % was adopted as drift limit for the IO performance level. The LS limit state is defined as the post-earthquake damage state in which a structure has damaged components but retains a margin against onset of partial or total collapse. Some structural elements may have severe damage, but this has not resulted in large falling debris hazards. When the wall drift ratio reached 2.5 %, nail connection failure was observed mainly near the sheathing corners, as shown in Fig. 3(a). The strain gages indicated that the yielding zones kept expanding in the steel members. The hybrid shear wall almost reached its peak capacity but still had enough remaining resistance and ductility. Therefore, the drift ratio of 2.5% can be adopted for the LS performance level for the hybrid shear wall system. The CP limit state in ASCE/SEI-41 is defined as the state that the structure has little residual stiffness and strength. Large permanent drifts may also occur, and infill walls may fail, which indicates the structure is near collapse. Fig. 3(b) shows the damage state in the infill wall when the drift ratio reached 5.0%. Entire nail connection lines failed due to edge tear-outs or fatigue fracture. Plastic hinges formed in most of the major steel members. Although the load carrying capacity of the hybrid shear wall system was greatly reduced, the hybrid system showed some ductile behavior and still had resistance against collapse. The drift ratio of 5.0% was adopted as the drift limit for the CP performance level in this study. However, the drift limit for the CP performance level may still require some further discussion based on more experimental investigations in future studies. As summary, the performance requirements for the timber-steel hybrid shear wall systems are given in Table 1 based on the test observations as well as the code provisions.

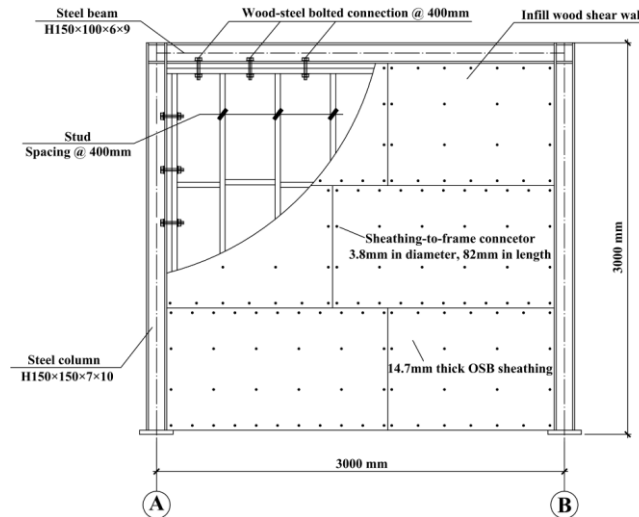


Fig. 4 Timber-steel hybrid baseline wall

3. Analysis

3.1 Hybrid baseline wall configuration

Fig. 4 shows the structural configuration of the tested hybrid shear wall, used as a baseline wall in this study. Mild carbon steel Q235B with a yielding strength of 235 MPa was used for the steel members. The cross sections of H-150×100×6×9 and H-150×150×7×10 (conforming to Chinese Standard GB 50017-2003) were used for beams and columns in the steel frame. For the infill wall, No. 2 and better grade Spruce-Pine-Fir (SPF) 38 × 140 mm dimension lumber with a spacing of 400 mm was used as framing members, and performance rated 19/32 APA grade OSB panels, with 1220 × 2440 mm in plane size and 14.7 mm in thickness, were used as the sheathing material. The panels were attached to the framing members with 3.8 × 82 mm spiral nails spaced at 150 mm on panel edges and 300 mm in field. M14 Bolts spaced at 400mm were used to connect the top plate and side studs of the infill wall to the steel frame. The shear force was transferred from the steel frame to the infill wood shear wall through these bolted connections, which ensured the integrity of the hybrid system.

3.2 Numerical model verification

A nonlinear finite element (FE) model was developed using ABAQUS software package by Li *et al.* (2013) to simulate the seismic response of the timber-steel hybrid shear walls. A specific feature of the numerical model was the implementation of a so-called “pseudo nail” algorithm as a user-defined subroutine to represent the hysteretic behavior of the infill wood shear walls. Considering the similar hysteretic characteristics between a wood shear wall and a nail connection, the “pseudo nail” model was proposed by Gu and Lam (2004) to represent the load-drift hysteresis of a wood shear wall using a nailed connection model. In this model, the model parameters need to

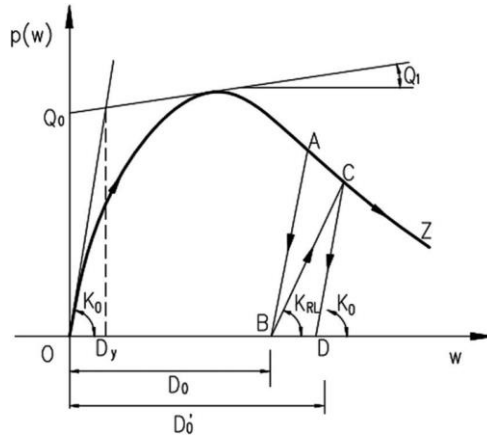


Fig. 5 Force-slip relationship of wood embedment in pseudo-nail model

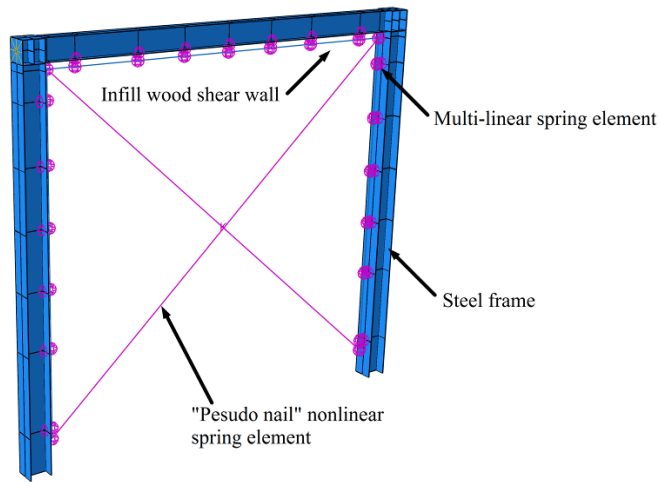


Fig. 6 Finite element model for the timber-steel hybrid shear wall system

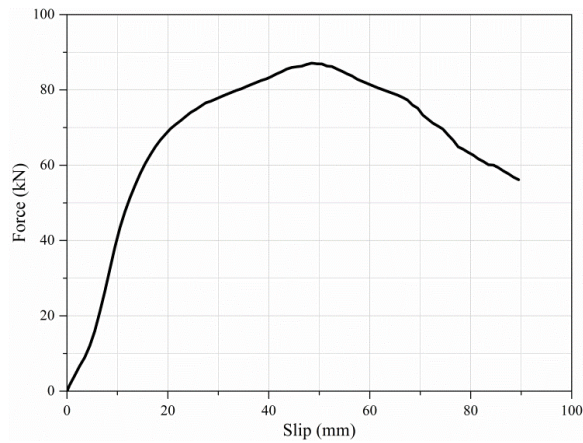


Fig. 7 Load-slip curve of bolted wood-steel connection

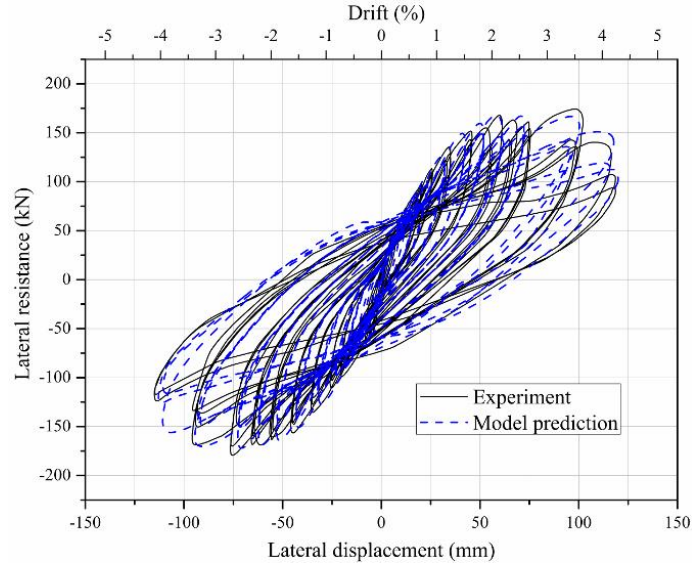


Fig. 8 Model prediction of hysteretic loops versus test results

be calibrated in order to match the magnitudes of shear wall forces and drifts. These parameters include the nail length L , diameter D and parameters to describe the compressive properties of the surrounding embedment medium, which is modeled as nonlinear compression-only springs with an exponential force-deformation relationship, $P(w)$. For the wood embedment part in the “pseudo nail” model, five parameters (Q_0 , Q_1 , Q_2 , K_0 , and D_{\max}) are used to define $P(w)$, as shown in Fig. 5 and Eqs. (1) - (3).

$$\begin{cases} P(w) = (Q_0 + Q_1 w)(1 - e^{-K_0 w/Q_0}) & \text{if } w \leq D_{\max} \\ P(w) = P_{\max} e^{Q_3 (w - D_{\max})^2} & \text{if } w \geq D_{\max} \end{cases} \quad (1)$$

where

$$P_{\max} = (Q_0 + Q_1 D_{\max})(1 - e^{-K_0 D_{\max}/Q_0}) \quad (2)$$

$$Q_3 = \frac{\log(0.8)}{[(Q_2 - 1.0)D_{\max}]^2} \quad (3)$$

It is assumed that the compressive behavior shows a peak (P_{\max}), followed by a softening trend.

Thus, $P(w)$ is represented by two exponential curves meeting at the peak load, as shown in Fig. 5. K_0 is the initial stiffness of the embedment relationship; Q_0 and Q_1 are the intercept and slope of the asymptote, respectively, as deformation w tends to infinity. However, w is constrained to not exceed a maximum (D_{\max}), at which $P(w)$ reaches P_{\max} . Q_2 gives the fraction of D_{\max} at which the pressure drops to 0.8 P_{\max} during the softening phase. The reloading from point B follows a straight line and with reduced stiffness K_{RL} , which can be defined according to the initial stiffness K_0 and the gap size (D_0). The details of the “pseudo-nail” model have been discussed elsewhere (Li *et al.* 2009). The “pseudo-nail” model has been shown to be very computationally efficient

under both static and dynamic loading (Gu and Lam 2004; Li *et al.* 2012a, 2012b), and it was believed to be more robust than the empirical curve-fitted models because, to some extent, it embodies the internal mechanism of a wood shear wall to resist lateral loads such as the interaction between wood medium and metal fasteners (Li *et al.* 2012c).

The FE model for the timber-steel hybrid shear wall system in ABAQUS is shown in Fig. 6. The infill wood shear wall was modeled by a wood frame and a pair of user defined “pseudo nail” spring elements. The wood frame was defined as pinned connected with no lateral stiffness, and the lateral performance of the wood shear wall was entirely represented by the “pseudo nail” springs. Multi-linear spring elements were used to model the bolted wood-steel connections. The load-slip relationship, as shown in Fig. 7, which was obtained from monotonic tests for the bolted wood-steel connections, was used as input for the multi-linear spring element. The steel frame was modelled by shell element (S4R), and the plastic behavior was adopted as combined hardening. The cyclic test results from He *et al.* (2013) were used to verify the numerical model. Fig. 8 shows that the model predictions agreed well with test results.

Table 2 Ground motion records used in analysis

| NO | Event | Station | R_{closest}^a (km) | Soil Type ^b | Component | PGA (g) |
|----|------------------------------|-------------------------------|--------------------------------|---------------------------|-----------|------------|
| 1 | Superstition Hills (1987) | Brawley | 18.2 | D | 315 | 0.116 |
| 2 | | El Centro Imperial | 13.9 | D | EW | 0.258 |
| 3 | | Plaster City | 21.0 | D | 135 | 0.186 |
| 4 | Northridge (1994) | Beverly Hills | 19.6 | C | NS | 0.416 |
| 5 | | Canoga Park | 15.8 | D | 106 | 0.356 |
| 6 | | Glendale-Las Palmas | 25.4 | D | 177 | 0.357 |
| 7 | | LA-Hollywood Storage | 25.5 | D | EW | 0.231 |
| 8 | | LA-North Faring Road | 23.9 | D | NS | 0.273 |
| 9 | | North Hollywood- Coldwater | 14.6 | C | EW | 0.271 |
| 10 | | Sunland-Mt Gleason Ave | 17.7 | C | 260 | 0.157 |
| 11 | Loma Prieta (1989) | Capitola | 14.5 | D | NS | 0.529 |
| 12 | | Gilroy Array No.3 | 14.4 | D | NS | 0.555 |
| 13 | | Gilroy Array No.4 | 16.1 | D | NS | 0.417 |
| 14 | | Gilroy Array No.7 | 24.2 | D | NS | 0.226 |
| 15 | | Hollister Diff. Array | 25.8 | D | 255 | 0.279 |
| 16 | | Saratoga-West Valley | 13.7 | C | EW | 0.332 |
| 17 | Cape Mendocino (1992) | Fortuna Boulevard | 23.6 | C | NS | 0.116 |
| 18 | | Rio Dell Overpass | 18.5 | C | EW | 0.385 |
| 19 | Landers (1992) | Desert Hot Springs | 23.3 | C | EW | 0.154 |
| 20 | | Yermo Fire Station | 24.9 | D | NS | 0.152 |

Note: ^a R_{closest} is the closest distance from the station to the fault rupture;

^bAccording to ASCE7-10 (2010), soil type C denotes a site with very dense soil and soft rock, and soil type D denotes a site with stiff soil.

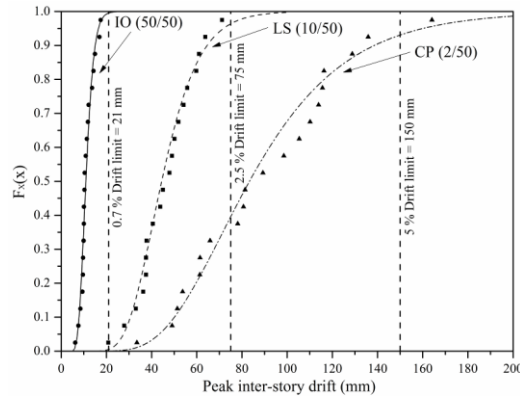


Fig. 9 Cumulative distribution function of peak inter-story drift for the baseline hybrid shear wall

3.3 Seismic input and distribution function

As listed in Table 2, a suite of 20 historical non-near-fault ground motion (OGM) records in southern California which were also used in the CUREE-Caltech Project (Krawinkler *et al.* 2000), were used to illustrate the procedure of constructing performance curves for the timber-steel hybrid shear walls. Seismic zone 4, which means the return period of the earthquake with a peak ground acceleration of 0.4 g is 500 years, was assumed. This procedure can be easily applied to other site conditions by using other earthquake ground motion records. The ground motions were scaled to seismic hazard levels via a response spectrum approach. For the LS limit state, each record was scaled such that its mean 5 % damped spectral value between periods of 0.10 sec and 0.60 sec matched ASCE/SEI-41 design spectral value of 1.1g for the same period. For the IO and the CP limit states, the records were scaled to their respective hazard levels in accordance with the provisions in the ASCE/SEI-41 and the IBC (2012) as well. For the hybrid shear wall located at the ground floor, the carried mass was estimated as 4500 kg/m according to the weight of a five-story residential building.

The cumulative distribution function (CDF) of peak wall drifts can be used to evaluate the probability of the wall drift response exceeding the performance criterion under a certain hazard level. It is quite convenient to estimate the probabilities of exceedance / non-performance with CDFs. In this study, the peak wall drifts from the nonlinear time-history analysis over the suite of earthquake ground motions were fitted to a lognormal (LN) distribution $F_X(x)$:

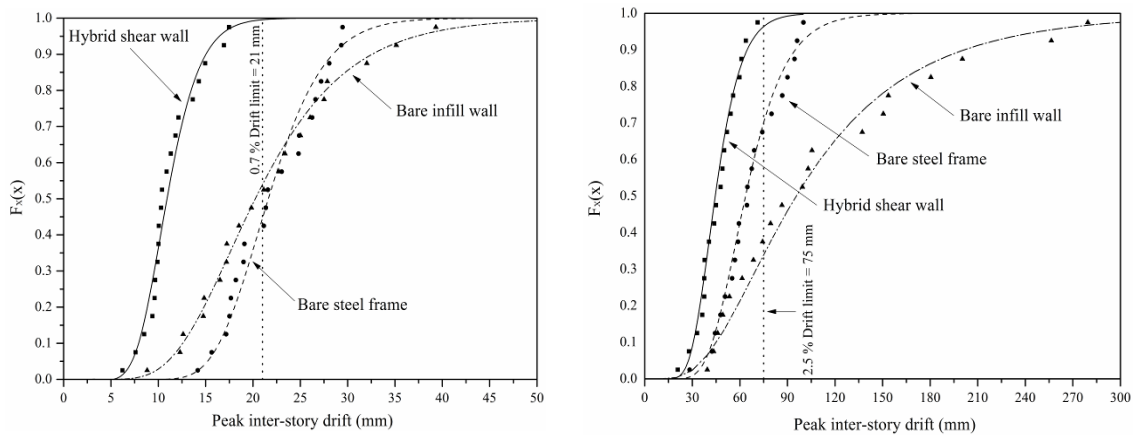
$$F_X(x) = \Phi\left(\frac{(\ln x - \lambda)}{\xi}\right) \tag{4}$$

where $\Phi(\square)$ = standard normal cumulative distribution function; λ and ξ are LN parameters, which can be obtained by a maximum likelihood procedure. Fig. 9 shows sample CDFs for the baseline wall under CP, LS and IO limit states. It is noted in Fig. 9 that the probability that the peak drift will exceed the drift limit for CP is 8% (92% non-exceedance probability), and the probability that the peak drift will exceed the drift limit for LS is 4% (96% non-exceedance probability). For IO limit state, the probability of non-performance of this hybrid shear wall is below 1% (about 99% non-exceedance probability).

4. Results and discussions

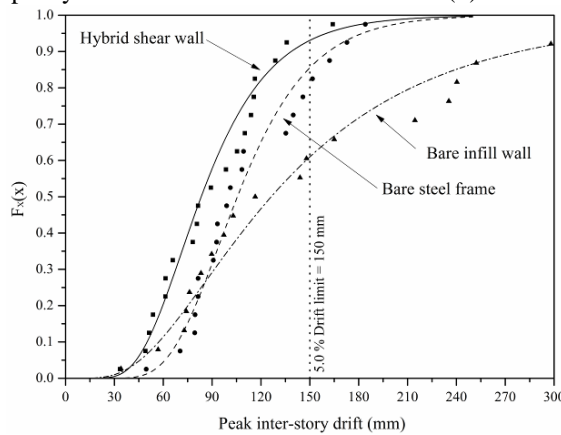
4.1 Influence of the infill wall

In the timber-steel hybrid shear walls, seismic load was simultaneously resisted by the steel moment frame and the infill wood shear wall. To study the effectiveness of the infill wall, the CDFs of the peak wall drift responses of the baseline hybrid shear wall, its corresponding bare steel frame and bare infill wood shear wall carrying the same amount of mass with respect to the IO, LS and CP limit states were established, respectively. For the IO limit state, as shown in Fig. 10(a), the non-performance probability was about 1% for the hybrid shear wall system and was about 60% and 46% for the bare steel frame and the bare infill wall, respectively. For the LS limit state, as shown in Fig. 10(b), the non-performance probability was 4% for the hybrid shear wall system, and was 30% and 66% for the bare steel frame and the bare infill wall, respectively. For



(a) Immediate occupancy limit state

(b) Life safety limit state



(a) Collapse prevention limit state

Fig. 10 Influence of the infill wall in the hybrid shear wall system

the CP limit state, as shown in Fig. 10(c), the non-performance probability was 8% for the hybrid shear wall system, and was 16% and 39% for the bare steel frame and the bare infill wall, respectively.

Apparently, the infill wall was very effective on reducing the shear wall drift responses with respect to these three seismic hazard levels. The infill wall seemed to be most effective in the hybrid system when ground shaking was not so severe. This was because the infill wall increased the initial wall stiffness significantly but was less ductile than the steel moment frame. As seismic load and wall deformation increased, the infill wall suffered more damage and reduced its contribution to load sharing. This also explains why the difference between the CDFs of the hybrid system and the bare steel frame with respect to the CP limit state was much smaller than that for the IO limit state. In general, the infill wood shear wall significantly increased the seismic reliability of the hybrid system, especially for IO and LS limit states.

4.2 Relative lateral infill to frame stiffness

Tong *et al.* (2005) revealed that for an infilled frame system, the relative lateral infill-to-frame stiffness ratio is an important parameter, which has a major influence on the loading sharing among the infill wall and the steel frame. The lateral stiffness ratio K_r can be defined as the ratio of the elastic stiffness between the infill wall and the steel frame:

$$K_r = k_{\text{infill}} / k_{\text{bf}} \quad (5)$$

where $k_{\text{infill}} = 0.4P_{\text{infill}} / \Delta_{\text{infill}}$ and $k_{\text{bf}} = 0.4P_{\text{bf}} / \Delta_{\text{bf}}$, P_{infill} is the peak load resisted by the infill wood shear wall; and Δ_{infill} is the infill wall drift at $0.4P_{\text{infill}}$; P_{bf} is the peak load resisted by the bare steel frame; and Δ_{bf} is the lateral displacement of the bare steel frame at $0.4P_{\text{bf}}$.

The K_r of the baseline hybrid wall was equal to 2.5. In this study, the seismic performance of hybrid shear walls with other K_r values was also evaluated. Hybrid walls with other K_r values (0.5, 1.0, and 5.0) were designed by changing the nailing and sheathing schedules of infill wood shear walls, as shown in Table 3. In all the walls, nail spacing was 150 mm on panel edges and 300 mm in field, and the bolted connections between the perimeter members of the wood infill wall and the steel moment frame were designed with sufficient stiffness to transfer the shear force between the steel frame and the infill wall. The K_r values from 0.5 to 5.0 represents a range of possible wood

Table 3 Structural configurations of infill walls for different relative lateral infill-to-frame stiffness ratios

| K_r | Nail type | Sheathing type | Sheathing pattern |
|-------|------------------------------|----------------|-------------------|
| 0.5 | CN50 ^a | 9.5mm OSB | One side |
| 1.0 | CN50 | 9.5mm OSB | Both sides |
| 2.5 | 12d common nail ^b | 14.7mm OSB | One side |
| 5.0 | 12d common nail | 14.7mm OSB | Both sides |

Note: ^aCN50 nail is confirmed to the Japanese Industrial Standards (JIS), with 50 mm in length and 2.87 mm in diameter.

^b12d common nail is confirmed to ASTM F1667-11a (Standard Specification for Driven Fasteners: Nails, Spikes, and Staples), with 82 mm in length and 3.8 mm in diameter

Table 4 Calibrated “Pesudo nail” model parameters for infill wood shear walls with different K_r values

| Parameter | $K_r = 0.5$ | $K_r = 1.0$ | $K_r = 2.5$ | $K_r = 5.0$ |
|-----------------------------|-------------|-------------|-------------|-------------|
| Q_0 (kN/mm) | 1.092 | 2.638 | 3.632 | 6.141 |
| Q_1 (kN/mm ²) | 0.005 | 0.004 | 0.004 | 0.005 |
| Q_2 (ratio) | 1.400 | 1.400 | 1.500 | 1.600 |
| K_0 (kN/mm ²) | 0.243 | 0.326 | 0.588 | 1.386 |
| D_{\max} (mm) | 87.501 | 76.801 | 44.212 | 51.542 |
| L (mm) | 200.00 | 200.00 | 300.00 | 300.00 |
| D (mm) | 4.00 | 5.00 | 6.50 | 9.50 |

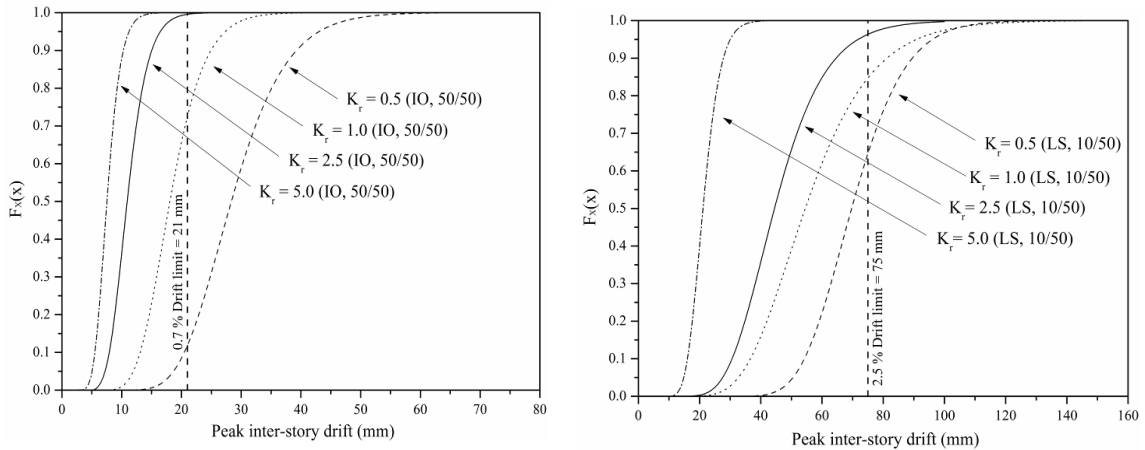
infill shear wall applications in steel moment frames, and the calibrated “pseudo nail” wall parameters are listed in Table 4.

The ABAQUS hybrid wall model was used to run the nonlinear time history analyses for these walls under the selected suite of ground motions. The peak drift responses for the hybrid systems with different K_r values are shown in Fig. 11. As expected, the infill-to-frame stiffness ratio was found to have a significant influence on the performance of the hybrid systems. For example, the non-performance probabilities under LS limit state were 33%, 15%, 4% and <1% for hybrid shearwalls with K_r values equaled to 0.5, 1.0, 2.5, and 5.0, respectively. The stronger infill-walls led to smaller peak drift responses. Therefore, the CDFs of the peak drift responses of the hybrid shear walls with K_r from 0.5 to 5.0 have shed some light on the influence of relative lateral infill-to-frame stiffness ratio on the seismic performance of the hybrid shear wall system under different seismic hazard levels.

4.3 Relative lateral infill to frame stiffness

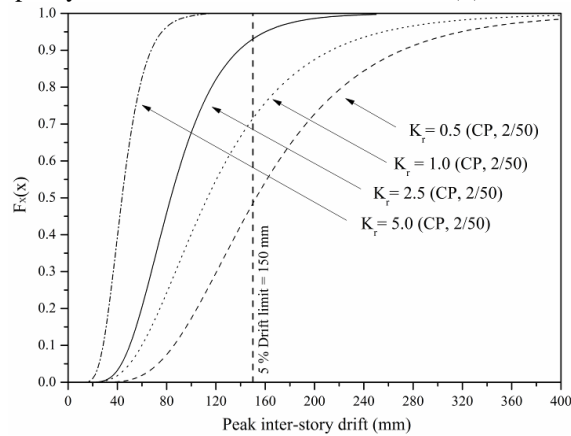
Previous studies on steel moment frames with concrete infill walls revealed that the load carrying capacity and stiffness of the infill-to-frame connections had a critical influence on the seismic performance of the hybrid systems. Similarly, in the timber-steel hybrid shear wall systems, the bolted connections between the perimeter wood framing members and the steel frame should be well designed to transfer the shear force along the timber-steel interfaces and ensure the load sharing between the two subsystems. The influence of bolt spacing on the lateral performance of the hybrid shear wall system was studied by the developed FE model. It was noted that the magnitudes of the shear force in the steel frames were quite similar among the hybrid shear walls. However, changes in spacing of the bolted connections mainly led to different infill wall behavior. Fig. 12 shows the shear force resisted by the infill wall with different bolted connection spacing. The shear force resisted by the infill wall dropped obviously as the connection spacing increased. In hybrid shear walls with larger bolt spacing (i.e., 1440 mm or 2880 mm), it was observed that the lateral load resisted by the infill wall dropped suddenly after the failure of bolted connections. The results indicated the effectiveness of the infill wall was closely related to the connections between wood and steel. In order to ensure the effectiveness of the infill wall, the connections must be capable of transferring the shear force equal to the ultimate load capacity of the infill wall.

In this study, as an example, the maximum shear forces in the bolted connections for the hybrid walls with different K_r value were obtained from the dynamic analyses. Fig. 13 shows the CDFs of these maximum shear forces. These curves were derived by considering “reliable” connections between wood and steel for all the hybrid shear walls, and this was done by modeling the bolted



(a) Immediate occupancy limit state

(b) Life safety limit state



(a) Collapse prevention limit state

Fig. 11 Peak inter-story drift of the hybrid shear walls with different relative infill-to-frame stiffness ratios

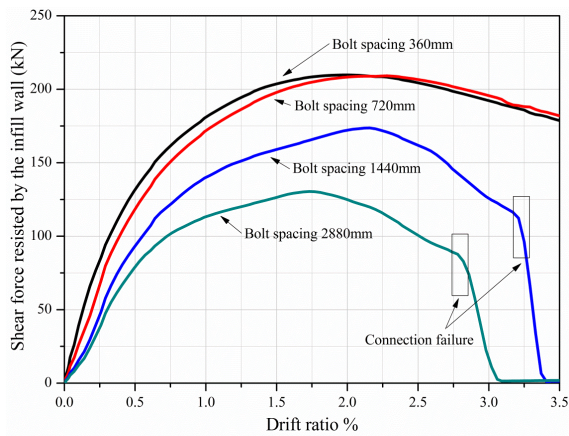


Fig. 12 Shear force resisted by the infill wall with various bolt spacing

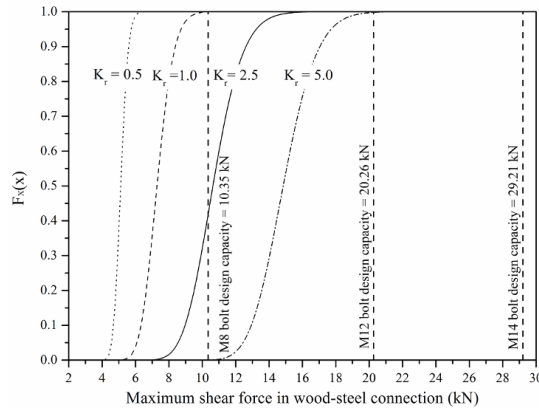


Fig. 13 Maximum shear force in bolted wood-steel connections under LS limit state

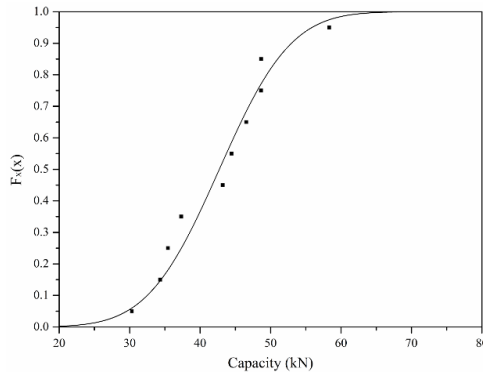


Fig. 14 Ultimate shear capacities from tests fitting to normal distribution

Table 5 Shear Capacities for Bolted Connections

| Bolt type | Average ultimate capacity (kN) | Design value (5th percentile) |
|-----------|--------------------------------|-------------------------------|
| M8 | 15.43 | 10.35 |
| M12 | 30.20 | 20.26 |
| M14 | 43.56 | 29.21 |

wood-steel connections through the same high stiffness springs for all the four hybrid shear walls. By doing this, the maximum shear force in the spring can be obtained in a dynamic analysis, and this maximum shear force is required to be transferred efficiently by the bolted wood-steel connections. Thus, for the four hybrid shear walls with different K_r values, their CDFs of maximum shear force in the springs can be coupled with the actual performance of bolted connections (i.e., M8, M12, and M14 design capacities in the figure), which allows structural engineers to select a bolt size which is capable of transferring the shear force efficiently for the hybrid shear wall with a specific K_r value.

Three types of bolts (M8, M12, and M14) were used to illustrate the selection of the bolted wood-steel connections. The bolts were confirmed to Chinese standard GB/T1231-2006. The maximum tensile stress of the bolts was between 830 and 1030 MPa. Monotonic loading tests

were conducted for the three types of timber-steel bolted connections. Each type of connection included 10 samples. The bolted connection's ultimate tension capacities were assumed to be normally distributed with mean values taken as the average ultimate tension capacities obtained from the tests. According to this information, the 5th-percentile value for load carrying capacity of each timber-steel bolted connection was determined and this characteristic value was treated as a capacity limit (design value) in this study. As an example, Fig. 14 shows the test results for ultimate capacity of the M14 bolted connections fitting to a normal distribution. Table 5 shows the mean and 5th percentile values for the timber-steel bolted connections.

The shear capacities for different bolt diameters are shown in Fig. 13. It is noted that, with non-exceedance probability of 95 %, the shear force required to be transferred by each bolted connection spaced at 400 mm in the hybrid system with $K_r = 5.0$ is 17.8 kN, which means M12 or M14 bolts should be selected for the connection. For the hybrid system with $K_r = 0.5$, however, the shear force required to be transferred by each bolted connection is only 5.7 kN, which indicates M8 bolts could be used in the wood-steel connection.

4.4 Performance curves

The performance curves for the timber-steel hybrid shear wall system were also constructed by varying the structural mass (from 1500 kg/m to 8500 kg/m, with an increment of 1000 kg/m). As an example, Fig. 15 shows the 99 %, 95 %, 90 %, 80 % and 50 % non-exceedance performance curves of the baseline hybrid shear wall under the LS and the IO limit states. These performance curves can be used directly in seismic design. Under the LS limit state, the maximum carried mass by the baseline hybrid shear wall was 4600 kg/m with a target peak drift non-exceedance probability of 95%. However, if the target non-exceedance probability increases to 99%, the carried mass shall not exceed 4020 kg/m; and if the target non-exceedance probability is 50%, which might be the case for temporary constructions, the carried mass shall not exceed 6650 kg/m.

The performance curves in Fig. 16 can be used to design the hybrid shear wall system when the carried mass is pre-determined. For example, If the carried mass is 6000 kg/m, considering target peak drift non-exceedance probability of 95% with respect to the LS limit state, the hybrid shear wall with $K_r = 5.0$ is required. Similarly, the performance curves for the shear forces in the wood-steel bolted connections under LS limit state were also constructed in Fig. 17. Given seismic mass, the corresponding shear force for the wood-steel bolted connections in the hybrid system with different K_r values can be obtained directly from the performance curves in order to satisfy the target non-exceedance probability. Other performance curves can also be constructed when considering different performance levels and target non-exceedance probabilities.

5. Conclusions

This paper presented a performance-based seismic analysis for a type of timber-steel hybrid shear wall systems which may gain more applications in multi-story timber-steel hybrid buildings in future. The performance requirements under different seismic hazard levels for the hybrid shear wall systems were first verified through a damage analysis based on experimental results of the hybrid systems. The contribution of the infill wood shear wall on the seismic performance of the hybrid shear wall systems was studied. It was found that the infill wood shear walls were very

effective on improving the seismic performance of the hybrid system. They were particularly effective with respect to the IO and the LS limit states compared to the CP limit state. The relative lateral infill-to-frame stiffness ratio also had a strong influence on the performance of the hybrid system, and the drift responses decreased significantly when stronger infill wood shear wall was used.

A seismic design procedure for the timber-steel hybrid shear walls was also developed. By running nonlinear time-history analyses on the hybrid shear wall systems under different seismic hazard levels, performance curves were established with respect to different target non-exceedance probabilities. Design charts were further constructed with regard to various carried seismic masses. Examples of the performance curves in terms of peak drift responses, seismic masses, and shear forces in the wood-steel bolted connections, were used to illustrate the design procedure. Of course, seismic performance of the timber-steel hybrid shear wall systems may also be related to other important structural parameters (e.g. the configuration of steel frame or panel layouts of the infill walls). Following the similar procedures, performance curves in terms of those parameters can be established and used to achieve the most appropriate design while satisfying the given non-exceedance probabilities.

Acknowledgments

The authors would like to acknowledge the National Natural Science Foundation of China for supporting this work with a research grant (Grant No. 51378382).

References

- ASCE 7-10. (2010), "Minimum design loads for buildings and other structures", American Society of Civil Engineers, Reston, VA.
- ASCE/SEI-41. (2006), "Seismic rehabilitation of existing buildings", American Society of Civil Engineers, Reston, VA.
- Buchanan, A.H., Deam, B., Fragiaco, M., Pampanin, S. and Palermo, A. (2008), "Multi-storey prestressed timber buildings in New Zealand", *Struct. Eng. Int.*, **18**(2), 166-173.
- Ceccotti, A., Sandhaas, C., Okabe, M., Yasumura, M., Minowa, C. and Kawai, N. (2013), "SOFIE project - 3D shaking table test on a seven-storey full-scale cross-laminated timber building", *Earthq. Eng. Struct. Dyn.*, **42**(13), 2003-2021.
- Chinese Standard GB 50017-2003, Ministry of Housing and Urban-Rural Development of the People's republic of China (MOHURD). (2003), "Code for design of steel structures", Beijing, China (in Chinese).
- Chinese Standard GB/T1231-2006, China Machinery Industry Federation. (2006), "Specifications of high strength bolts with large hexagon head, large hexagon nuts, plain washers for steel structures", Beijing, China (in Chinese).
- Dickof, C., Stierner, S.F. and Tesfamariam, S. (2012), "Wood-steel hybrid seismic force resisting systems: seismic ductility", *Proceeding of the 12th World Conference on Timber Engineering, WCTE2012*, Auckland, New Zealand.
- Filiatrault, A. and Folz, B. (2002), "Performance-based seismic design of wood frame buildings", *J. Struct. Eng.*, **128**(1), 39-47.
- Frangiaco, M., Dujic, B. and Sustersic, I. (2011), "Elastic and ductile design of multi-storey crosslam massive wooden buildings under seismic actions", *Eng. Struct.*, **33**(11), 3043-3053.

- Gu, J. (2006), "An efficient approach to evaluate seismic performance and reliability of wooden shear walls", Ph.D Thesis, University of British Columbia, Vancouver, Canada.
- Gu, J. and Lam, F. (2004), "Simplified mechanics-based wood frame shear wall model", *Proceeding of the 13th World Conf. on Earthquake Engineering*, Paper No. 3109. Vancouver, Canada.
- He, M., Li, Z., Lam, F., Ma, R. and Ma, Z. (2013), "Experimental investigation on lateral performance of timber-steel hybrid shear wall systems", *J. Struct. Eng.*, (10.1061/(ASCE)ST.1943-541X.0000855).
- IBC. (2012), *2012 International Building Code*, International Code Council, Washington, D.C.
- Kazantzi, A.K., Righiniotis, T.D. and Chryssanthopoulos, M.K. (2008), "Fragility and hazard analysis of a welded steel moment resisting frame", *J. Earthq. Eng.*, **12**(4), 596-615.
- Kazantzi, A.K., Righiniotis, T.D. and Chryssanthopoulos, M.K. (2011), "A simplified fragility methodology for regular steel MRFs", *J. Earthq. Eng.*, **15**(3), 390-403.
- Kim, J.H. and Rosowsky, D. (2005). "Fragility analysis for performance-based seismic design of engineered wood shearwalls", *J. Struct. Eng.*, **131**(11), 1764-1773.
- Kinali, K. and Ellingwood, B. (2007), "Seismic fragility assessment of steel frames for consequence-based engineering: A case study for Memphis, TN", *Eng. Struct.*, **29**(6), 1115-1127.
- Krawinkler, H., Parisi, F., Ibarra, L., Ayoub, A. and Medina, R. (2000), "Development of a testing protocol for wood frame structures", CUREE Publication No. W-02, Consortium of Universities for Research in Earthquake Engineering, Richmond, California.
- Li, M., Lam, F. and Foschi, R.O. (2009), "Seismic reliability analysis of diagonal-braced and structural-panel-sheathed wood shear walls", *J. Struct. Eng.*, **135**(5), 587-596.
- Li, M., Lam, F., Foschi, R.O., Nakajima, S. and Nakagawa, T. (2012a), "Seismic performance of post-and-beam timber buildings I: model development and verification", *J. Wood Sci.*, **58**(1), 20-30.
- Li, M., Lam, F., Foschi, R.O., Nakajima, S. and Nakagawa, T. (2012b), "Seismic performance of post-and-beam timber buildings II: reliability evaluations", *J. Wood Sci.*, **58**(2), 135-143.
- Li, M., Foschi, R.O. and Lam, F. (2012c), "Modeling hysteretic behavior of wood shear walls with a protocol-independent nail connection algorithm", *J. Struct. Eng.*, **138**(1), 99-108.
- Li, Z., He, M., Lam, F., Li, M., Ma, R. and Ma Z. (2013), "Finite element modeling and parametric analysis of timber-steel hybrid structures", *Struct. Des. Tall Spec. Build.*, 2013, DOI: 10.1002/tal.1107.
- Pang, W., Rosowsky, D., Pei, S. and van de Lindt, J.W. (2010), "Simplified direct displacement design of six-story woodframe building and pretest seismic performance assessment", *J. Struct. Eng.*, **136**(7), 813-825.
- Sakamoto, I., Kawai, N., Okada, H., Yamaguchi, N., Isoda, H. and Yusa, S. (2004), "Final report of a research and development project on timber-based hybrid building structures", *Proceeding of the 8th World Conf. on Timber Engineering*, WCTE2004, Lahti, Finland.
- Smith, T., Fragiaco, M., Pampanin, S. and Buchanan, A. (2009), "Construction time and cost estimates for post-tensioned multi-storey timber buildings", *Proceeding of the Institutions of Civil Engineers, Construct. Mater.*, **162**(4), 141-149.
- Tong, X., Hajjar, J.F., Schultz, A.E. and Shield, C.K. (2005), "Cyclic behavior of steel frame structures with composite reinforced concrete infill walls and partially-restrained connections", *J. Constr. Steel Res.*, **61**(4), 531-552.
- Van de Lindt, J.W., Pei, S., Pryor, S.E., Shimizu, H. and Isoda, H. (2010), "Experimental seismic response of a full-scale six-story light-frame wood building", *J. Struct. Eng.*, **136**(10), 1262-1272.
- Wang, C. and Wen, Y. (2000), "Evaluation of pre-Northridge low-rise steel buildings. II: reliability", *J. Struct. Eng.*, **126**(10), 1169-1176.
- Zhou, L., Chen, Z., Chui, Y.H., Ni, C. and Asiz, A. (2012), "Seismic performance of mid-rise light wood frame structure connected with reinforced masonry core", *Proceeding of the 12th World Conference on Timber Engineering*, WCTE2012, Auckland, New Zealand.